Available online at www.sciencedirect.com
SCIENCE DIRECT®
BioSystems 73 (2004) 57–71
BioSystems
www.elsevier.com/locate/biosystems

Time hierarchies in the *Escherichia coli* carbohydrate uptake and metabolism

A. Kremling*, S. Fischer, T. Sauter, K. Bettenbrock, E.D. Gilles

Systems Biology Group, Max-Planck-Institut für Dynamik Komplexer Technischer Systeme, Sandtorstr. 1, 39106 Magdeburg, Germany

Received 23 April 2003; received in revised form 24 July 2003; accepted 2 September 2003

Abstract

The analysis of metabolic pathways with mathematical models contributes to the better understanding of the behavior of metabolic processes. This paper presents the analysis of a mathematical model for carbohydrate uptake and metabolism in *Escherichia coli*. It is shown that the dynamic processes cover a broad time span from some milliseconds to several hours. Based on this analysis the fast processes could be described with steady-state characteristic curves. A subsequent robustness analysis of the model parameters shows that the fast part of the system may act as a filter for the slow part of the system; the sensitivities of the fast system are conserved. From these findings it is concluded that the slow part of the system shows some robustness against changes in parameters of the fast subsystem, i.e. if a parameter shows no sensitivity for the fast part of the system, it will also show no sensitivity for the slow part of the system.

Keywords: Phosphotransferase system; Time scale separation; Sensitivity analysis; Robustness; PEP/pyruvate ratio

1. Introduction

With developments in new measurement technologies, and therefore the availability of time courses for intracellular metabolites, the set up and validation of mathematical models for cellular systems (or parts of the metabolism) has become very popular. Detailed mathematical models promise a better understanding of the system under investigation, i.e. the models can be used for prediction and design and it might be possible to draw new conclusions in fields of application like biotechnology and medical science (Kremling et al., 2001b). These activities are summarized with the keyword "systems biology" and a number of projects mainly in the US (Agrawal, 1999, but also in Japan (Kitano, 2000)) have now begun.

In this contribution, we concentrate on a very important part of the bacterial regulatory system. The phosphotransferase system (PTS) is an uptake system for several carbohydrates in *Escherichia coli*. Besides this, it acts as a sensor and is involved in the control of uptake of a number of carbohydrates. For example, if glucose is present in the medium, the synthesis of many other C-source transport proteins and their corresponding catabolic enzymes is repressed. Since the PTS represents the start of the signal transduction pathway, the understanding of its dynamics is fundamental for the understanding of the whole pathway. Mathematical models for the PTS can be found in a number of contributions. Liao et al. (1996) present a simple approach covering all steps in one equation. Rohwer et al. (2000) discuss a very detailed model including all reaction steps. They analyze the steady-state behavior of the system and present results using metabolic control analysis (MCA). Recent studies take diffusion

* Corresponding author. Tel.: +49-391-6110-466.
E-mail address: kre@mpi-magdeburg.mpg.de (A. Kremling).

0303-2647/$ – see front matter © 2003 Elsevier Ireland Ltd. All rights reserved.
doi:10.1016/j.biosystems.2003.09.001

into account (Francke et al., 2002). In Kremling et al. (2001a) the reaction equations are divided into three modules: the first module describes the activities of the general PTS proteins EI and HPr, the second module describes the phosphotransfer from HPr to EIIA^{Crr} and the third module describes the actual transport step mediated by the glucose transporter EIICB^{Glc}.

Here, we have investigated carbohydrate uptake and metabolism on different time scales. The work was motivated by findings with laboratory experiments; a "pulse response" experiment revealed fast dynamics while diauxic growth on glucose plus lactose covered a broader time scale. Experiments were performed either with a genetically engineered sucrose positive strain or a wild type strain. The sucrose positive strain was used during the pulse response experiment. A mathematical model describing sucrose uptake and metabolism was introduced previously (Wang et al., 2001). Measurements of a pulse response experiment were used to identify parameters of the glycolysis and the phosphotransfer reactions of the PTS. The wild type strain was used to identify parameters involved in the control of glucose and lactose uptake. Since the work focuses on model analysis, the experimental findings are only summarized briefly.

For model analysis, only glucose uptake and metabolism are under consideration. A close relationship between time-scale hierarchies and robustness was pointed out in Rojdestvenski et al. (1999). Robustness is the insensitivity of a selected characteristic time course of a component, network function to sustain growth (Stelling et al., 2002, adaption precision (Barkai and Leibler, 1997)) with respect to changes of external or internal parameters (different environmental conditions, mutations, or altered kinetic parameters). Rojdestvenski et al. (1999) conclude that the decoupling of a system into two subsystems is necessary for robustness. Running on different time-scales is one of the characteristics that allow such decoupling. A robustness analysis of the overall system was performed to check the results of Rojdestvenski et al. (1999).

2. *Escherichia coli* sugar uptake and metabolism

The PTS represents a transport and at the same time a signal transduction system responsible for carbon catabolite repression and inducer exclusion (Postma et al., 1993). In a set of five reactions, a phosphoryl group is transferred from phophoenolpyruvate (PEP) through two common intermediates, enzyme I (EI, gene *ptsI*) and the phosphohistidine carrier protein (HPr, gene *ptsH*), to the EII^{Glc}, and finally to the substrate (see Fig. 1 for the glucose PTS). EII^{Glc} consists of the soluble EIIA^{Crr} (gene *crr*, hereafter denoted as EIIA) and the membrane-bound transporter EIICB^{Glc} (gene *ptsG*) for glucose uptake. The Scr-PTS possesses a sucrose-specific membrane-bound transporter EIIBC^{Scr} (gene *scrA*), which also receives the phosphoryl group from EIIA. For further description of the PTS, see Postma et al. (1993). All proteins involved in this phosphorylation cascade act as signaling molecules, e.g. EI in chemotaxis, HPr in glycogen metabolism, and EIIA in inducer exclusion (by inhibition of lactose transport by the lactose permease LacY). The incoming phosphorylated form of the sugar is further metabolized: Glycolysis is the link between the transport reactions and their energy supply. Metabolism of glucose 6-phosphate during glycolysis results in two moles of PEP.

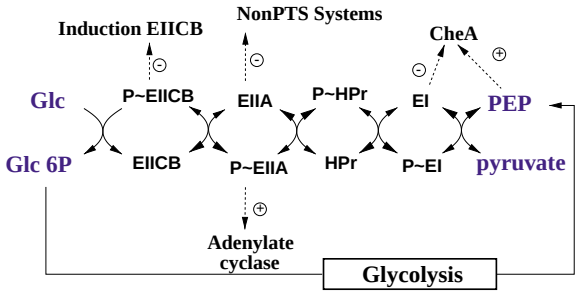

Fig. 1. Schematic representation of the Glc-PTS. Inputs are the entire concentrations of EI, HPr, EIIA, EIICB, PEP, pyruvate, and extracellular glucose. Important outputs are the phosphorylated and unphosphorylated forms of EIIA. These two conformations are measured in several experiments. Solid lines represent metabolic reactions and dashed lines signal outputs of the PTS.

PTS-protein synthesis is under control of at least two regulators. While the cAMP·Crp complex acts as an activator (DeReuse and Danchin, 1988), Mlc is a repressor for *ptsG*, *ptsHI* and *crr* (Plumbridge, 1998). If glucose is present in the medium, EIICB^{Glc} is mainly in its dephosphorylated form. This form binds Mlc, and therefore prevents it from binding to the operator binding site (Tanaka et al., 2000; Lee et al., 2000).

3. Experimental results

The work was motivated by experiments performed in our laboratory. They were used as a basis for this study. Material and methods are according to Kremling et al. (2001a). The work was performed either with the wild type strain LJ110 (Zeppenfeld et al., 2000) or with LJ210. LJ210 (laboratory collection of K. Jahreis, Osnabrück) is a Scr^+ derivative of LJ110 that carries chromosomally the *scr* genes of pUR400 (Wohlieter et al., 1975; Schmid et al., 1982).

3.1. Pulse response experiment

To characterize the dynamic behavior of the glycolysis in interaction with the PTS, the response of the cells in steady-state to environmental disturbances was examined. In the experiments, we cultivated *E. coli* LJ210 in a continuous fermentation in a CSTR (type KLF2000, volume 2.0l, Bioengineering) with defined minimal medium as described in Kremling et al. (2001a). The disturbance of the culture in steady-state (dilution rate $D = 0.1\,h^{-1}$, concentration of sucrose in the feed $c_{in} = 17\,g/l$) was performed by injection of a concentrated sucrose solution to a final concentration of 0.3 g/l. Resulting time courses of the fraction of unphosphorylated EIIA, and glycolysis metabolites (glucose 6-phosphate, fructose, fructose 6-phosphate, PEP, and pyruvate) were measured as described elsewhere (Ishizuka et al., 1993; Takahashi et al., 1998; Bergmeyer, 1979). The obtained trajectories are shown in Fig. 2. Note that during continuous culture, the steady-state condition $D = \mu$ holds true, where μ is the specific growth rate. Under the chosen experimental conditions, cells are sugar limited.

The added sucrose is consumed within 200 s. Gene expression can be neglected for this short time interval. The pulse can be followed in all measured glycolysis metabolites. The concentration of PEP decreases because of increased consumption for the transport process via the sucrose PTS. The important signaling component EIIA is totally dephosphorylated, and returns to the former steady-state after depletion of the added sucrose.

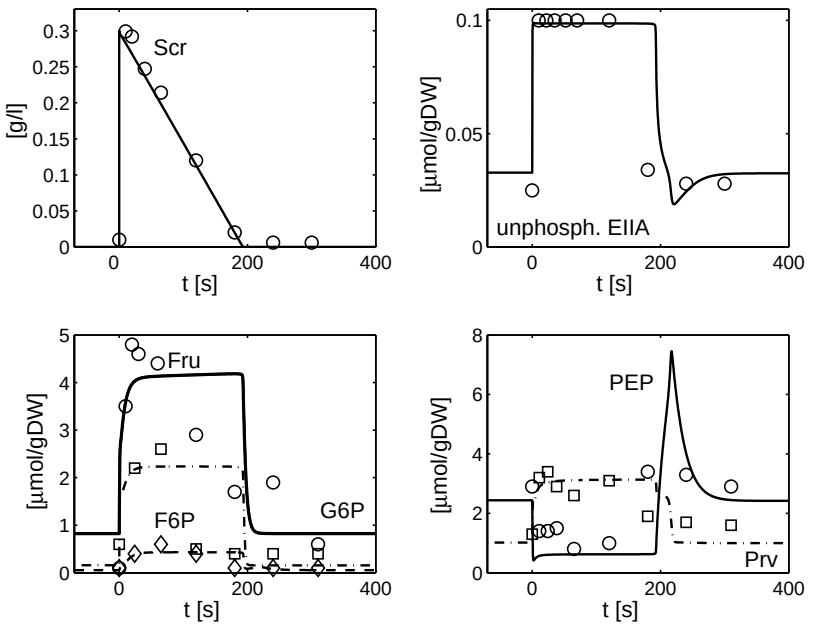

Fig. 2. Dynamic response of the PTS and glycolysis to a sucrose pulse disturbing a continuous culture in steady-state ($D = 0.1\,h^{-1}$). The extracellular sucrose concentration was increased abruptly at $t = 0$ s to a final concentration of 0.3 g/l. Experimental results are represented by marks, simulation results by lines.

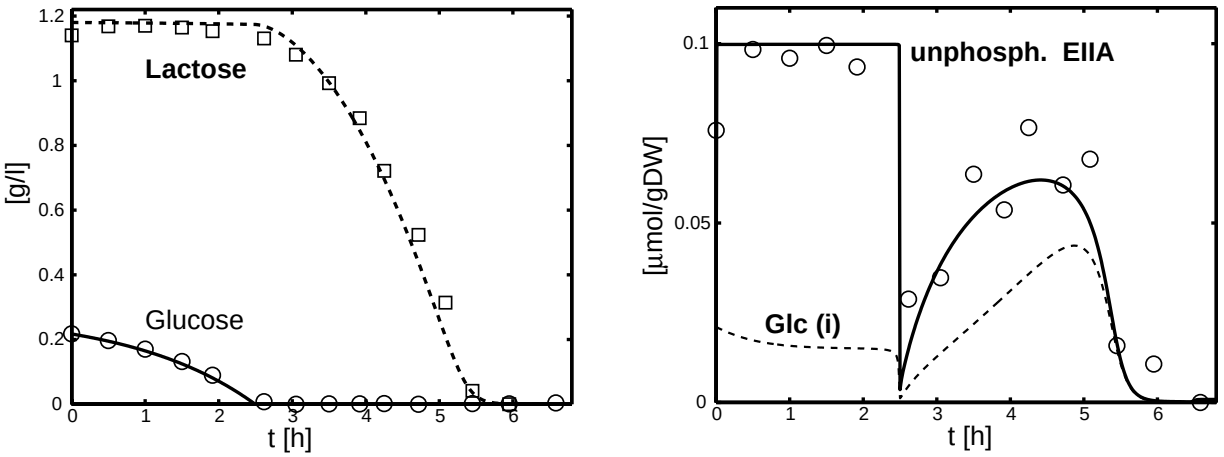

Fig. 3. Left: Time course of glucose and lactose in the medium during diauxic experiment. Right: Time course of the intracellular protein concentration of unphosphorylated EIIA and simulated intracellular glucose (dashed values were multiplied by factor 20). Experimental results are represented by marks, simulation results by lines.

3.2. Diauxic growth on two substrates

The growth of strain LJ110 in mixed cultures with glucose and lactose was characterized to analyze effects of gene expression on the dynamics of the PTS. Fig. 3 shows simulations and experimental results for extracellular glucose and lactose as well as for unphosphorylated EIIA when both carbohydrates are present in the medium at the beginning. In addition, model prediction for intracellular glucose is also shown.

As expected for the glucose phase, protein EIIA is mainly unphosphorylated. After the glucose is consumed, EIIA shifts very quickly to its phosphorylated form (representing fast dynamics) and subsequently becomes more and more unphosphorylated. This is probably because intracellular glucose may also be phosphorylated by the PTS. The observed dephosphorylation of EIIA can be interpreted as regulatory phenomenon; since EIIA is an uncompetitive inhibitor of the lactose permease LacY, the increase of unphosphorylated EIIA leads to a reduced lactose uptake rate. This prevents accumulation of glycolytic intermediates during high lactose uptake rates.

4. Model equations for the PTS and glycolysis

Model analysis will focus on glucose uptake and metabolism. Therefore, only the equations for the glucose PTS are discussed here.

4.1. Glucose PTS

The following reaction steps are incorporated into the model. Phosphoryl transfer from PEP to EI (dimer) is described by:

$$\mathrm{EI} + \mathrm{PEP} \underset{k_{-1}}{\overset{k_1}{\rightleftharpoons}} \mathrm{P} \sim \mathrm{EI} + \mathrm{Prv}, \tag{1}$$

where Prv stands for pyruvate. There is no evidence that dimerization of EI plays a role in the dynamics of the PTS for the investigations performed in this paper. The dimer is the most important conformation and is the only conformation considered here. Transfer of a phosphoryl group to HPr is described by:

$$\mathrm{P} \sim \mathrm{EI} + \mathrm{HPr} \underset{k_{-2}}{\overset{k_2}{\rightleftharpoons}} \mathrm{EI} + \mathrm{P} \sim \mathrm{HPr}. \tag{2}$$

Phosphoryl transfer from HPr to EIIA is described by:

$$\mathrm{P} \sim \mathrm{HPr} + \mathrm{EIIA} \underset{k_{-3}}{\overset{k_3}{\rightleftharpoons}} \mathrm{HPr} + \mathrm{P} \sim \mathrm{EIIA}. \tag{3}$$

Since protein EIICB^{Glc} is membrane bound and since it is not clear if there is sequential binding of EIIA and the carbohydrate or a random binding (a carbohydrate molecule is able to bind to the unphosphorylated enzyme), a random kinetic rate law is used for the last two steps of the PTS; phosphoryl transfer from EIIA and the phosphorylation of the incoming carbohydrate (intracellular glucose is not included in the model, be-

cause it is assumed that the concentration is very low at all conditions used here):

$$\mathrm{P} \sim \mathrm{EIIA} + \mathrm{Glc_{ex}} \xrightarrow{r_4} \mathrm{EIIA} + \mathrm{Glc} \sim \mathrm{P}, \tag{4}$$

with the rate law r_4 for glucose is taken from Kremling et al. (2001a):

$$r_4 = \frac{k_4 c_{\mathrm{EIICB0}} c_{\mathrm{P\sim EIIA}} c_{\mathrm{Glc}}}{(K_{\mathrm{EIIA}} + c_{\mathrm{P\sim EIIA}})(K_{\mathrm{Glc}} + c_{\mathrm{Glc}})}. \tag{5}$$

4.2. Glycolysis

To get a clear picture of the dynamics, a simplified model of glycolysis was used since the number of time constants is equal to the number of observables. The model comprises one step summarizing glycolytic reactions and drain into the monomers starting from glucose 6-phosphate, PEP, and pyruvate. Glycolysis in the simple model is described by:

$$\mathrm{G6P} \xrightarrow{r_{\mathrm{gly}}} 2\mathrm{PEP}. \tag{6}$$

The pyruvate kinase reaction is as follows:

$$\mathrm{PEP} \xrightarrow{r_{\mathrm{pyk}}} \mathrm{Prv}. \tag{7}$$

Furthermore, drain into monomer synthesis has been taken into account by the following reaction scheme:

$$\begin{aligned} &\mathrm{G6P} \rightharpoonup^{r_{\mathrm{dr1}}} \text{biosynthesis} \\ &\mathrm{PEP} \rightharpoonup^{r_{\mathrm{dr2}}} \text{biosynthesis} \\ &\mathrm{Prv} \rightharpoonup^{r_{\mathrm{dr3}}} \text{biosynthesis}. \end{aligned} \tag{8}$$

All reaction rates for the model described so far are summarized in Appendix A. As shown below, gene expression is responsible for very slow dynamics of the phosphorylated PTS components. For the analysis of the slow dynamics the lactose uptake system and its control by the cAMP·Crp complex are included from Kremling et al. (2001a). Since lactose is split into glucose and galactose, the intracellular glucose pool depends strongly on the concentration of the lactose permease and β-galactosidase. In the model, intracellular glucose can be phosphorylated by the PTS as well as by a glucokinase (gene *glk*).

4.3. Model parameters

A rough structure of the whole model is given in Fig. 4. The model differs from Kremling et al. (2001a) in the PTS equations and the simplified model for glycolysis. To estimate parameters from the presented data, a procedure used in Kremling et al. (2001a) was applied. (i) Starting with parameters from literature (Rohwer et al., 2000), a sensitivity analysis was performed to detect the most sensitive parameters. (ii) Together with the measured data and the Fisher information matrix (Ljung, 1999) it was determined, whether the sensitive parameters could be estimated, or not. Using a method introduced by Posten and Munack (1990) a set of parameters from the sensitive parameters that could be estimated together were determined. Parameters for the PTS and glycolysis are summarized in Table 1. Differences between the original model Kremling et al. (2001a) and the model presented here are negligible (data not shown).

The underlying reaction scheme for the PTS used here is simpler than that presented by Rohwer et al.

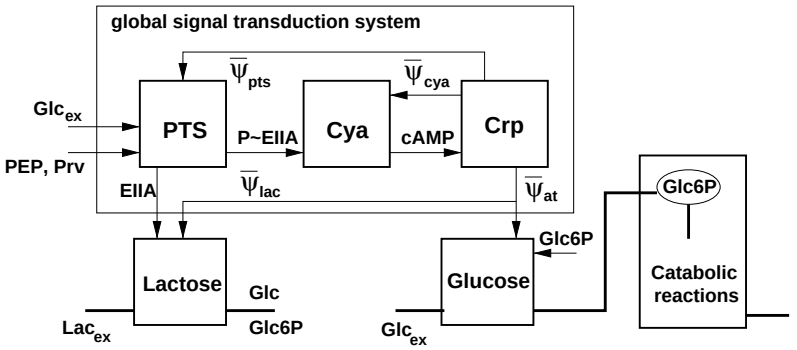

Fig. 4. Functional units in the *crpA*-modulon. Protein EIIA and its phosphorylated form P∼EIIA are the main output signals of the Glc-PTS. The output signals $\bar{\psi}$ from the CrpA submodel describe the transcription efficiency of the genes and operons under control of the cAMP·CrpA complex (Kremling and Gilles, 2001).

Table 1
Summary of the model parameters of the PTS and the simplified glycolysis

PTS		Glycolysis	
k_1	8.9E+6 gDW/μmol	k_{gly}	6500 μmol/gDW h
k_{-1}	5.9E+6 gDW/μmol h	K_{G6P}	1.5 μmol/gDW
k_2	2.8E+7 gDW/μmol h	k_{pyk}	1000.0 μmol/gDW h
k_{-2}	2.5E+7 gDW/μmol h	K_{PEP}	100.0 μmol/gDW
k_3	5.0E+6 gDW/μmol h	k_{g6p}	1500.0 1/h
k_{-3}	7.5E+6 gDW/μmol h	k_{pep}	200.0 1/h
k_4	9.17E+6 gDW/μmol h	k_{pyv}	25370 1/h
K_{EIIA}	0.0085 μmol/gDW		
K_{Glc}	0.0012 g/l		
c_{EI0}	0.012 μmol/gDW		
c_{HPr0}	0.12 μmol/gDW		
c_{EIIA0}	0.1 μmol/gDW		
c_{EIICB0}	0.003 μmol/gDW		

(2000). Model parameters were fitted using experimental results from Wang et al. (2001) and our own as yet unpublished experimental results. Therefore, the number of (uncertain) parameters was kept as low as possible. Since different strains and experimental conditions were used, one cannot expect the parameters to show a good agreement with parameters from literature. This is reflected, for example, by calculating the overall equilibrium constant K_{eq} for the first three reactions steps of the PTS:

$$K_{eq} = \frac{c_{P\sim EIIA}}{c_{EIIA}} \frac{c_{Prv}}{c_{PEP}}. \quad (9)$$

Here a value $K_{eq} = 1.13$ is obtained while the value from Rohwer et al. (2000) is $K_{eq} = 48.7$ and from Hogema et al. (1998) is $K_{eq} = 14.0$. The overall concentrations for the PTS proteins are fixed. For the experiment shown in Fig. 3, the value for c_{EIICB0} was taken from a simulation study with the model from Kremling et al. (2001a). The model takes into account that the synthesis of EIICB is under control of Mlc and the cAMP·Crp complex while the values for the other PTS proteins are taken as constants. In contrast, Rohwer et al. (2000) used constant concentrations of all PTS proteins.

5. Model analysis

Model analysis by means of theoretical tools is useful for a better understanding of the behavior of cellular systems. In silico, models are characterized by a large number of elements and interactions, i.e. the order of the system is rather high. However, systems running on different time-scales tend to couple the behavior of the fast modes to the slow modes. Algebraic equations can be used for the fast modes, if a steady-state is assumed. Furthermore, the influence of the parameters on the behavior of the system is important. Here, a sensitivity analysis is used to detect important model parameters.

5.1. Time-scale separation

First, we analyzed the time hierarchies for the conditions given during the "pulse response" experiment. Therefore, the eigenvalues and eigenvectors of a subsystem including PTS and glycolysis (observables EI, HPr, EIIA, G6P, PEP, and Prv) were calculated. To determine eigenvalues and eigenvectors a steady-state for $r = 1.1$ mmol/gDW h was chosen, representing the condition used in the experiment. The equations are linearized around the steady-state and the Jacobian J is obtained. A transformation of the old system observables $\underline{x}$ into new coordinates $\underline{z}$ with the inverse of the matrix of eigenvectors T^{-1}

$$\underline{z} = T^{-1}\underline{x}, \quad (10)$$

allows an analysis of the system in separate time windows characterized by the eigenvalues. Fig. 5 shows the entries of the rows of T^{-1} where the abscissa represents the observables of the original system. Plots A–C represent very fast processes. To detect the main components of one mode, the linearized system was stimulated by a step in the glucose concentration. Afterwards, the entries in the lines of T^{-1} must be multiplied with the concentrations of the respective observables. For line 1 in T^{-1}, representing the fastest mode, the main components are EI, Prv, HPr and PEP. These observables are involved in the first PTS reaction. In the second mode, the main components are HPr and EIIA, which are involved in the second PTS reaction. A clearer picture emerges when a new mode can be directly linked to one of the observables of the original system. This is the case for mode z_4, representing the dynamics of glucose 6-phosphate and mode z_5, representing the dynamics of pyruvate. The slowest mode, z_6, represents the dynamics of two original observables, namely PEP and glucose 6-phosphate.

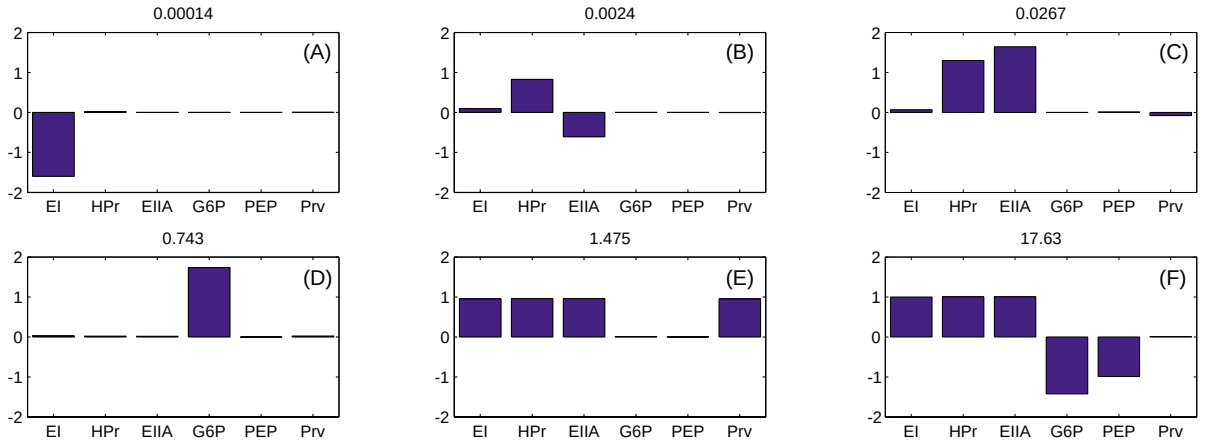

Fig. 5. Eigenvectors of the simplified reaction scheme for a glucose uptake rate of $r = 1.11$ mmol/gDW h (rows of the matrix T^{-1}). The headline of each plot gives the apparent time constant of the system in (s).

To verify the results for the group translocation through the PTS proteins EI, HPr, and EIIA, we simulated the first second(s) of the pulse response experiment with the nonlinear model. The time courses of the PTS proteins, glucose 6-phosphate, pyruvate and PEP as well as the time courses of the PTS rates (r_1, r_2, r_3, r_4) are shown in Fig. 6. Based on the estimated model parameters the rate of glucose uptake (r_4) varies with time. After a very fast increase it is not possible to maintain at this rate, since r_1, r_2, and r_3 are slower and the supply with phosphoryl groups could not be satisfied immediately, even though enough energy in form of PEP is available. This is in agreement with the simulation results of the intracellular concentrations of the PTS proteins; the concentration of phosphorylated EIIA shows a quick drop, because it transfers the phosphoryl groups to glucose. In contrast, the concentrations of phosphorylated EI and HPr drop slower. All PTS components reach a steady-state within 5 s. After the PEP pool is replenished by glycolytic reactions the uptake rate of the PTS rises again and reaches a steady-state after 30 s.

With respect to gene expression, PTS and glycolysis have much smaller time constants. The overall transport rate in this case reads

$$r = f(c_{\mathrm{PEP}}, c_{\mathrm{Prv}}, c_{\mathrm{carbo}}, c_{\mathrm{EIIBC0}}, c_{\mathrm{EIIA0}}, c_{\mathrm{EI0}}, c_{\mathrm{HPr0}}), \tag{11}$$

which is the solution of the algebraic equation system, setting all time derivatives of the observables to zero. Fig. 7 summarizes the steady-state behavior of the system. The glycolytic metabolites—other than PEP—increase with increasing uptake rate while the fractions of the phosphorylated PTS components EIIA and EI decrease with an increasing uptake rate. The half maximal uptake rate was detected in the range of 0.23 mg/l (1.3 μM). The value is smaller than in other reports, perhaps reflecting in vivo conditions.

5.2. Robustness analysis

Rojdestvenski et al. (1999) stated, that the sensitivities of the fast part of the system are conserved when the dynamics of the remainder slow subsystem is analyzed. To check the assumption, a robustness analysis was performed. This was done by calculating changes of the time course of a selected observable with respect to changes in the kinetic parameters, i.e. by calculating the parameter sensitivities. This means that the slow subsystem shows some robustness against parameter changes, i.e. if a parameter shows no sensitivity for the fast subsystem, it will show no sensitivity for the slow subsystem.

Several methods are available to calculate and analyze parameter sensitivities defined by:

$$w_{ij} = \frac{\partial x_i}{\partial p_j}, \tag{12}$$

where x_i is a observable of the model and p_j is a model parameter. A very popular method is used in

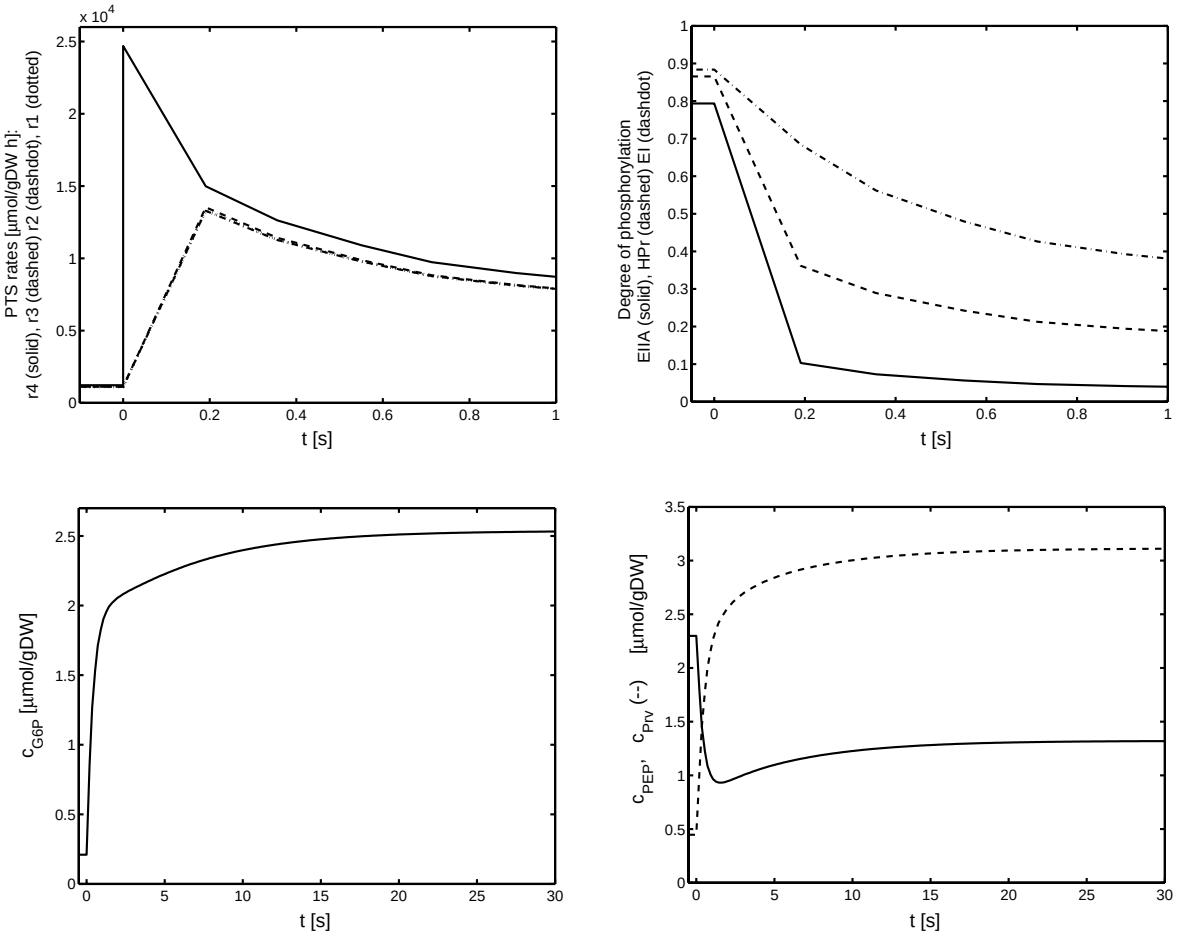

Fig. 6. Time course of the simulated PTS rates, the degree of phosphorylation of the PTS proteins, and selected intracellular metabolites (glucose 6-phosphate second row left, PEP, pyruvate second row right). For discussion of the dynamic behavior, see text.

Metabolic Control Analysis (e.g. see Heinrich and Schuster, 1996). The method uses several theorems to connect local sensitivities and to make a statement on global sensitivities and therefore relates the systemic behavior to local properties. Here, a method from Hearne (1985) developed for dynamic systems was applied. Hearne (1985) suggests finding the direction in which the overall parameter vector should be perturbed, so as to maximize the disturbance to the trajectories of interest. In contrast to other approaches, the method of Hearne (1985) integrates the sensitivities of selected parameters on selected observables. The method is also useful when looking for parameters that are able to alter specific observables for which measurements are available.

The method is based on the formulation of the following optimization problem:

$$\max \sum_{i=1}^{n} \sum \frac{\Delta x_i}{x_i} \Delta t, \tag{13}$$

with observables x_i and changes Δx_i of x_i due to changes $\Delta \boldsymbol{p}$ of parameter vector $\boldsymbol{p}$. The dimension of the system is n. The solution can be found by calculating the maximal eigenvalue and corresponding eigenvector of matrix $\boldsymbol{G}$ given in Appendix A. To calculate matrix $\boldsymbol{G}$, dynamic and algebraic equations for the sensitivities have to be solved. For a differential-algebra (DA) system with dynamic observables $\underline{x}$, algebraic observables $\underline{z}$, and parameter vector $\underline{p}$ of the general

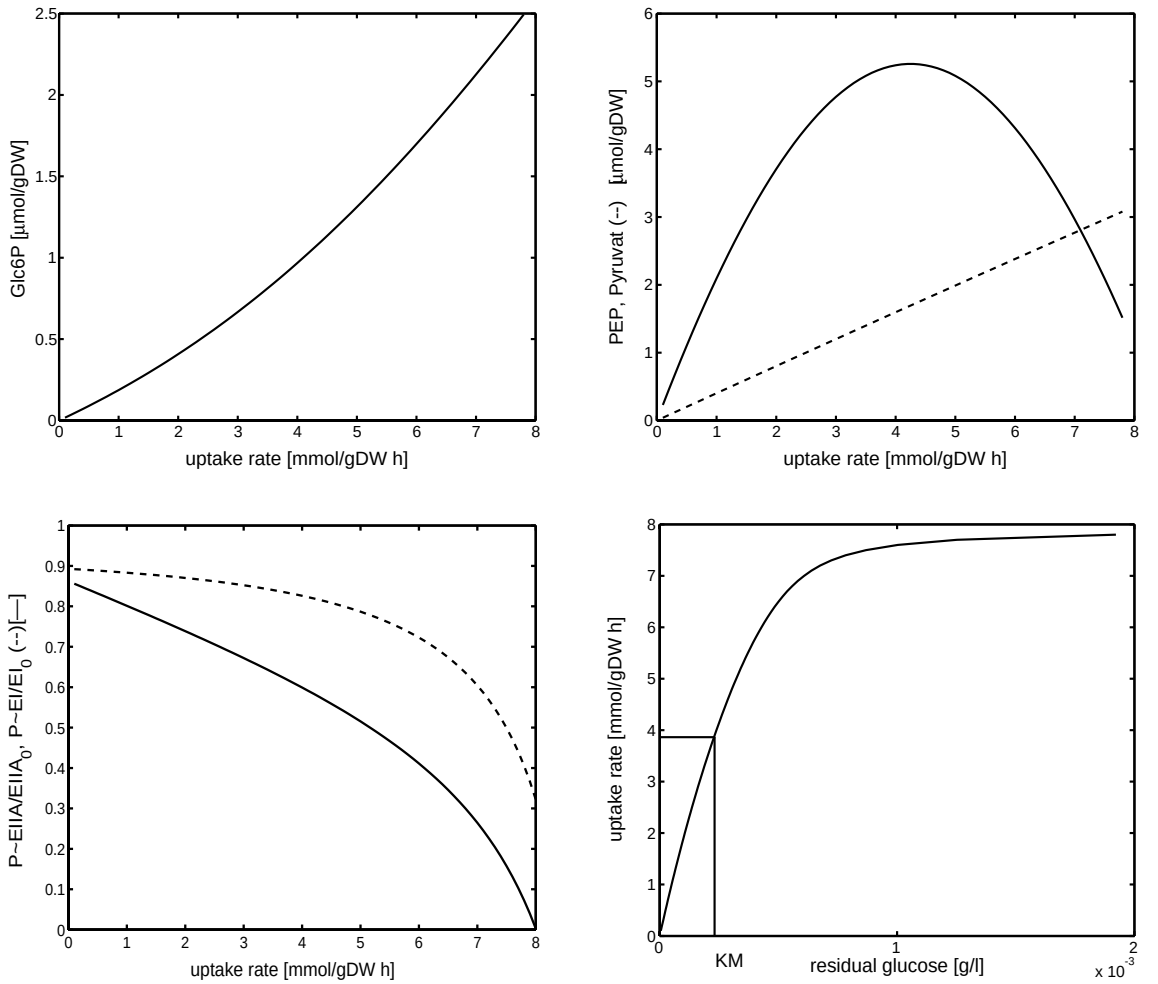

Fig. 7. Steady-state behavior of the PTS/glycolysis model. Glucose 6-phosphate (upper-left plot); PEP and pyruvate (upper-right plot: PEP solid, pyruvate dashed); fraction of phosphorylated EIIA and EI (lower-left plot: EIIA solid, EI dashed); uptake rate vs. residual glucose concentration (lower-right plot). The half maximal glucose uptake rate is achieved with 0.23 mg/l.

form:

$$\dot{\underline{x}} = \underline{f}(\underline{x}, \underline{z}, \underline{p}) \tag{14}$$

$$\underline{0} = \underline{g}(\underline{x}, \underline{z}, \underline{p}), \tag{15}$$

the matrix of the non-normalized sensitivities $W_x = (\mathrm{d}\underline{x}/\mathrm{d}\underline{p})$ and $W_z = (\mathrm{d}\underline{z}/\mathrm{d}\underline{p})$ can be calculated by the two following equations:

$$\dot{W}_x = \frac{\mathrm{d}\underline{f}}{\mathrm{d}\underline{p}} + \frac{\mathrm{d}\underline{f}}{\mathrm{d}\underline{x}} W_x + \frac{\mathrm{d}\underline{f}}{\mathrm{d}\underline{z}} W_z \tag{16}$$

$$0 = \frac{\mathrm{d}\underline{g}}{\mathrm{d}\underline{p}} + \frac{\mathrm{d}\underline{g}}{\mathrm{d}\underline{x}} W_x + \frac{\mathrm{d}\underline{g}}{\mathrm{d}\underline{z}} W_z. \tag{17}$$

For the analysis in this contribution the following strategy is used:

- The model is separated into two parts: a *fast* part and a remainder *slow* part. Based on the analysis above, observables and parameters are assigned to the respective parts.
- For the *fast* submodel, the sensitivity is calculated with the method of Hearne (1985), taking all observables and all parameters for the *fast* subsystem into account. This represents a "fingerprint" of the *fast* subsystem. The fingerprint is compared with the sensitivity of the same set of parameters, but now

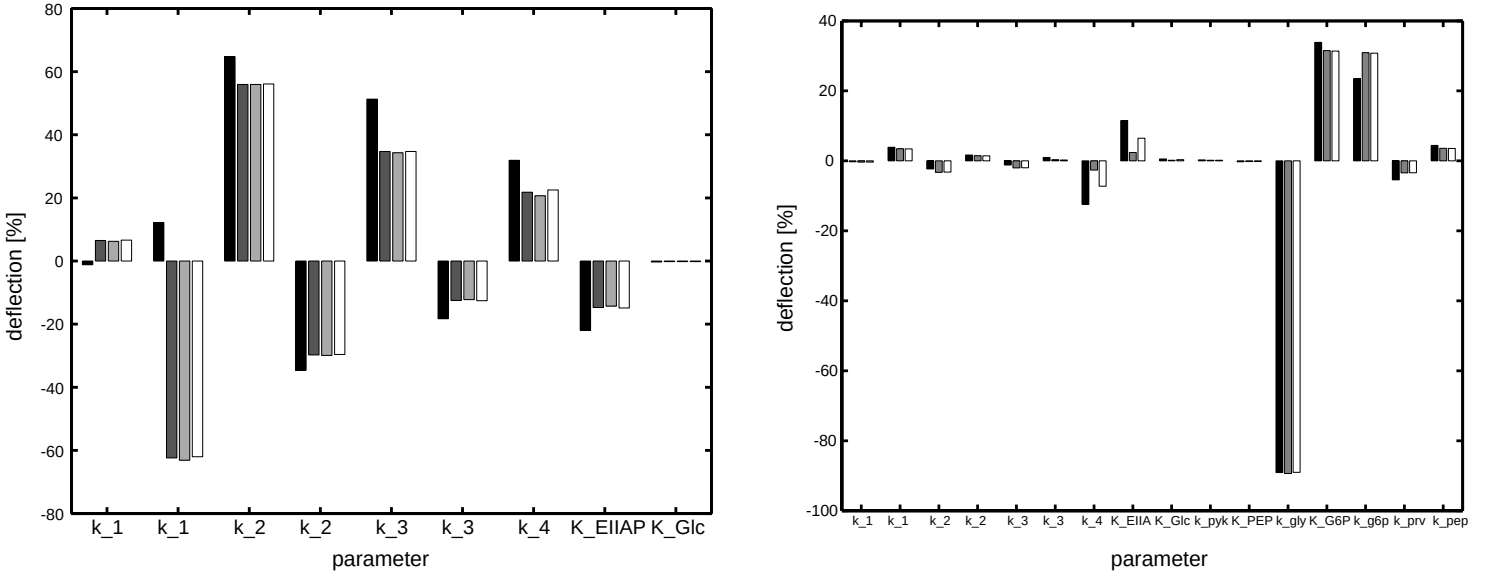

Fig. 8. Left-hand side: Case I: Fingerprint (black), glucose 6-phosphate (dark gray), PEP (light gray), pyruvate (white). With the exception of parameters k_1 and k_{-1}, the vector of perturbation of fingerprint is comparable to the selected observables of the slow subsystem. Right-hand side: Case II: Fingerprint (black), biomass (dark gray), LacZ (white). For all parameters the sensitivity of the fast system (fingerprint) is conserved for selected slow observables.

with respect to selected observables of the *slow* part of the system.

5.2.1. Case study I: pulse experiment

The fast part of the system is represented by the observables of the PTS (EI, HPr, EIIA), while the slow part of the system comprises glycolytic reactions. For the pulse experiment gene expression can be neglected, due to the short period of time. For the slow part, observables glucose 6-phosphate (vector of perturbation is dark gray), PEP (light gray), and pyruvate (white) are selected (Fig. 8, left-hand side). Except for parameters k_1 and k_{-1}, the vectors are comparable, although the values for the fingerprint are slightly higher in all other cases.

5.2.2. Case study II: diauxic growth experiment

Here the fast subsystem is represented by the observables of the PTS (EI, HPr, EIIA) and the glycolysis (G6P, PEP, and Prv). The remainder system is the slow part. Fig. 8, right-hand side, summarizes the results. As representatives of the slow part, the entire biomass (vector of perturbation is dark gray) and the lactose splitting enzyme LacZ (white) are selected. For all observables the sensitivity of the slow system is conserved in the fast system. The sensitivity of glycolysis is the most important.

6. Discussion

A mathematical model for glucose uptake and metabolism is analyzed with respect to time hierarchies and robustness. Based on previous published results, simplified versions for the subsystems PTS and glycolysis are used during this study.

6.1. Dynamics

It was shown that the structure of the PTS with its successive phosphorylation steps with different dynamics can lead to temporally shifted dephosphorylation of the PTS components. A very common tool in engineering science is the analysis of the eigenvalues and eigenvectors of the linearized system. Thereby the system is transformed in new coordinates. Every coordinate reaches a steady-state with a time constant that is represented by the reciprocal of the absolute value of the respective eigenvalue. The analysis indicates that the three fastest modes reach a steady-state with time constants smaller than $\tau = 0.03$ s. It was not possible to assign one of these modes directly to one of the original observables. Palsson and Lightfoot (1984) showed that a mode may also represent an equilibrium condition. The simulation results in Fig. 6 show that this is not the case for the PTS rates. The steady-state condition at the beginning of the experiment is very close to the equilibrium (in the equilibrium all rates are zero) and shifts away after the glucose pulse. In contrast to the fast modes, the main components of the slow modes z_4 and z_5 could be assigned directly to one observable of the original system: glucose 6-phosphate and pyruvate, respectively. However, simulaton results show that the time constants cannot be detected with the nonlinear model. Although the concentration of glucose 6-phosphate rises very quickly, a steady-state is reached after 30 s that is much slower than expected from the linearized model.

Experimental data for the time course of PEP are presented in Hogema et al. (1998): the PEP concentration decreases by a factor of ≈30 within 15 s after stimulation and increases during a period of 2 min, which is slower than shown here. This might also be due to the different experimental conditions and strains used. The experiment shown in Fig. 2, which is the basis for the parameter estimation, starts under limiting conditions (the initial steady-state is reached after 2 days) while Hogema et al. (1998) performed the experiment with cells taken from the exponential growth phase. Considering the glucose uptake rate, we get the remarkable result that the maximal value is nearly 25 mmol/gDW h, showing the very high capacity of the transporter.

Based on the results above, the analysis of the linear model show that the observables of the model can be divided into two groups. One group representing PTS reactions and a second group representing glycolytic reactions. But, the linear model can give only hints on the time constants of the system. Simulation studies with the nonlinear model are therefore necessary. Including slower processes such as gene expression in the analysis, the findings indicate that the slow increase of the unphosphorylated form of EIIA during the diauxic growth experiment can be explained by a slow accumulation of intracellular glucose during lactose metabolism. As can be seen in Fig. 9, the

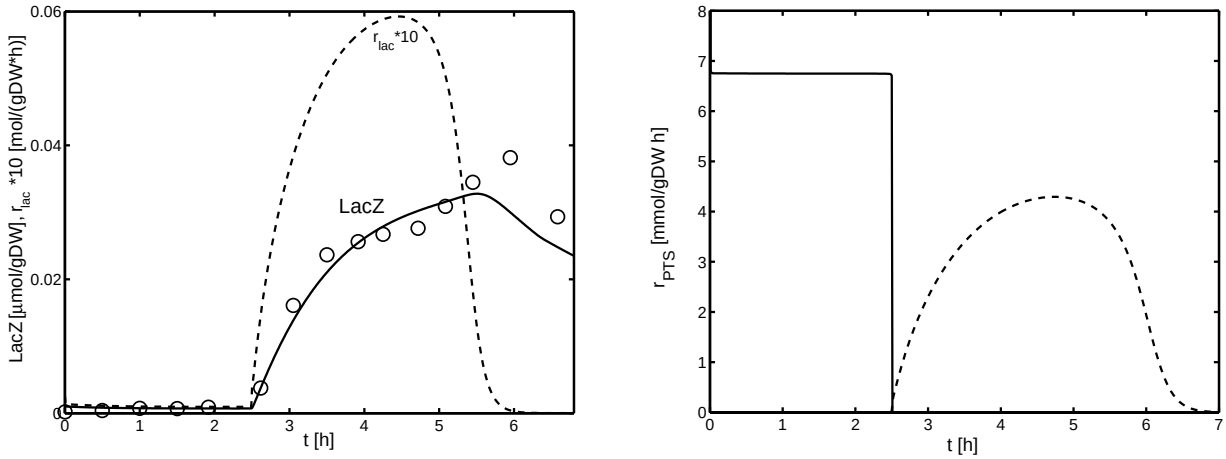

Fig. 9. Left: Time course of β-galactosidase (simulation and experimental results) and simulation of the rate of protein synthesis. Right: Uptake rate of glucose (solid), rate of phosphorylation of intracellular glucose (dashed).

induction of the *lac* operon lasts several hours, until a plateau is reached. Therefore, the rate through the PTS also rises slowly.

6.2. Steady-state characteristics

Regarding the steady-state characteristics, the degrees of phosphorylation of the PTS proteins EIIA and EI are nearly linear over a broad range (Fig. 7). For high uptake rates, the slope of the curve is decreasing, indicating a saturation behavior. This can also be seen in the plot of uptake rate versus glucose residual concentration. The values of PEP pass through a maximum at an uptake rate of 4 mmol/gDW h (close to the half maximal uptake rate), while glucose 6-phosphate and pyruvate show a linear dependency from the uptake rate. The initial values measured for PEP and pyruvate by Hogema et al. (1998) for glucose (6.8 and 2.2 µmol/gDW, respectively) are the same order of magnitude as those shown in the figure. The course of PEP reflects the very important role of this key metabolite in the entire system. For low uptake rates the PEP pool increases with increasing uptake rate, showing that PEP is available in sufficient amounts. For high uptake rates, the capacity of the glycolysis becomes more and more limiting, leading to decreasing PEP concentrations.

Since the degree of phosphorylation of protein EIIA is involved in the control of many carbohydrate transport systems, we calculated the degree of phosphorylation in dependency of the PEP/pyruvate ratio for the case where the PTS is active, and the case where the PTS is not active and a flux through glycolysis is enforced. When the PTS is not active the synthesis of pyruvate is realized only by the pyruvate kinase reaction. In Fig. 10 the pyruvate kinase flux was varied between 2 and 6 mmol/gDW h (the incoming flux to glucose 6-phosphate was fixed at 5 mmol/gDW h). As can be seen, the PEP/pyruvate ratio is decreasing with increasing pyruvate kinase flux. The right-hand side plot shows the shift of the degree of phosphorylation of EIIA in the cases where the PTS is active or not active. When the PTS is not active, from Eq. (9) the following equation will hold true for the degree of phosphorylation d_P:

$$d_P = \frac{c_{P\sim EIIA}}{c_{EIIA0}} = \frac{c_{PEP}/c_{Prv}}{1/K_{eq} + c_{PEP}/c_{Prv}}, \qquad (18)$$

showing that the curve does not depend on the overall amount of the PTS proteins. Note that Eq. (18) also represents the upper bound for the case that the PTS is active. This upper bound is reached if the concentration of the PTS proteins is increased.

The results of the model are in agreement with data in Hogema et al. (1998) (Fig.2 therein shows

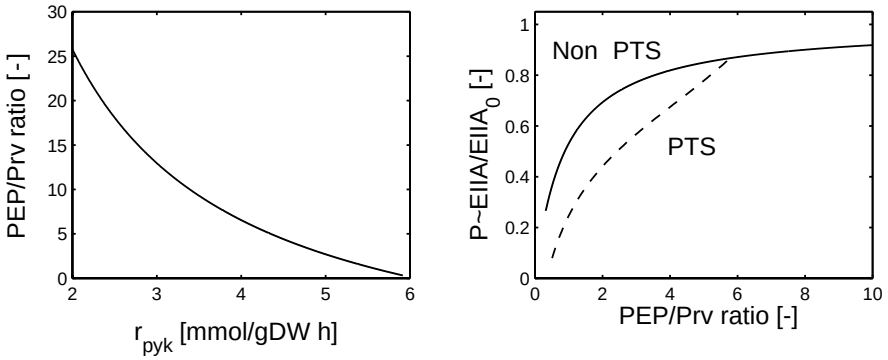

Fig. 10. Left: PEP/pyruvate ratio corresponding to the rate of pyruvate kinase when the PTS is not active. Right: Corresponding degree of phosphorylation for protein EIIA in the case that the PTS is not active (solid) and in the case where the PTS is active (dashed).

the degree of phosphorylation of EIIA for various carbon sources). Depending on the PEP/pyruvate ratio, the degree of phosphorylation is adjusted: For non-PTS sugars, e.g. glucose 6-phosphate, a low PEP/pyruvate ratio will also result in a low degree of phosphorylation, and therefore in low cAMP concentrations. If a non-PTS sugar is provided, the pyruvate kinase activity must be increased to establish the low PEP/pyruvate ratio. Data from literature indicates that the pyruvate kinase activity and concentration can be enhanced in a feed-forward loop by fructose 1,6-bis-phosphate (protein synthesis is under control of FruR, which is modified by fructose 1,6-bis-phosphate). Possibly, this results in a higher flux through pyruvate kinase if a high flux through glycolysis is possible, and therefore decreases the PEP/pyruvate ratio. Besides the pyruvate kinase activity other PEP metabolizing enzymes can also be expected to alter there activity in response to changes of the glycolytic flux and thereby also influence the PEP/pyruvate ratio. All findings indicate that for all sugars that feed into glycolysis, a high PEP/pyruvate ratio always points to a hunger situation, while a low PEP/pyruvate ratio signals a satisfactory situation.

6.3. Robustness

A new approach was introduced to analyze parameter sensitivities of slow and fast subsystems. The method calculates a vector of parameters that shows a maximal deflection of selected trajectories. These vectors are analyzed with respect to fast and slow observables of the model. The analysis of two experiments—pulse response and diauxic growth—reveals that some of the system parameters show a robust behavior: If a parameter shows no sensitivity in the fast system, it almost always show no sensitivity for slow observables. Therefore, it is concluded that the fast system may act as a kind of filter for the sensitivities. These findings may lead to an improvement during parameter identification for large systems composed of different units processing on different time scales. In the first example, the sensitivities are distributed on a number of parameters, showing that there is no single “bottleneck” in the PTS. For the second example discussed above (Case study II), it turns out that the glycolytic flux, represented by parameter k_{gly}, shows the highest sensitivity for the slow variables, e.g. biomass and LacZ. Since the slow processes reflect control of protein synthesis, e.g. via P $\sim$ EIIA, the importance of the glycolytic flux discussed already above and observed by Hogema et al. (1998) is confirmed from a theoretical point of view.

From research in microbiology, the PTS is designed as a sensor system. From our results and the cited experimental studies, it is concluded that it is a sensor system for external carbon source supply, but rather the glycolytic flux and the PEP/pyruvate ratio show a sensor function while the PTS acts more as a transmitter to process the signal to synthesize cAMP and finally activates Crp to start transcription.

Appendix A

A.1. Model equations for the simplified PTS/glycolysis model

The following rates are defined for reactions (1)–(3):

$$r_1 = k_1 c_{\mathrm{PEP}} c_{\mathrm{EI}} - k_{-1} c_{\mathrm{Prv}} (c_{\mathrm{EI0}} - c_{\mathrm{EI}}) \tag{A.1}$$

$$r_2 = k_2 c_{\mathrm{HPr}} (c_{\mathrm{EI0}} - c_{\mathrm{EI}}) - k_{-2} c_{\mathrm{EI}} (c_{\mathrm{HPr0}} - c_{\mathrm{HPr}}) \tag{A.2}$$

$$r_3 = k_3 c_{\mathrm{EIIA}} (c_{\mathrm{HPr0}} - c_{\mathrm{HPr}}) - k_{-3} c_{\mathrm{HPr}} (c_{\mathrm{EIIA0}} - c_{\mathrm{EIIA}}), \tag{A.3}$$

and the model equations read, together with Eq. (5):

$$\begin{aligned} \dot{c}_{\mathrm{EI}} &= -r_1 + r_2 \\ \dot{c}_{\mathrm{HPr}} &= -r_2 + r_3 \\ \dot{c}_{\mathrm{EIIA}} &= -r_3 + r_4. \end{aligned} \tag{A.4}$$

For glycolysis the following kinetics are used:

$$r_{\mathrm{gly}} = k_{\mathrm{gly}} \frac{c_{\mathrm{G6P}}}{K_{\mathrm{G6P}} + c_{\mathrm{G6P}}} \tag{A.5}$$

$$r_{\mathrm{pyk}} = k_{\mathrm{pyk}} \frac{c_{\mathrm{PEP}}}{K_{\mathrm{PEP}} + c_{\mathrm{PEP}}} \tag{A.6}$$

$$r_{\mathrm{dr1}} = k_{\mathrm{g6p}} c_{\mathrm{G6P}} \tag{A.7}$$

$$r_{\mathrm{dr2}} = k_{\mathrm{pep}} c_{\mathrm{PEP}} \tag{A.8}$$

$$r_{\mathrm{dr3}} = k_{\mathrm{prv}} c_{\mathrm{PRV}}, \tag{A.9}$$

and the equation system read:

$$\begin{aligned} \dot{c}_{\mathrm{G6P}} &= r_4 - r_{\mathrm{gly}} - r_{\mathrm{dr1}} \\ \dot{c}_{\mathrm{PEP}} &= -r_1 + 2 \times r_{\mathrm{gly}} - r_{\mathrm{pyk}} - r_{\mathrm{dr2}} \\ \dot{c}_{\mathrm{Prv}} &= r_1 + r_{\mathrm{pyk}} - r_{\mathrm{dr3}}. \end{aligned} \tag{A.10}$$

A.2. Method of Hearne (1985)

The method of Hearne (1985) uses the normalized sensitivities ω_{ij}

$$\omega_{ij} = w_{ij} \frac{p_j}{x_i} = \frac{\partial x_i}{\partial p_j} \frac{p_j}{x_i},$$

$$\boldsymbol{\Omega} = \begin{bmatrix} \omega_{11} & \dots & \omega_{1m} \\ & \dots & \\ \omega_{n1} & \dots & \omega_{nm} \end{bmatrix}, \tag{A.11}$$

and the vector of sensitivities $\boldsymbol{s}$

$$\boldsymbol{s} = \begin{bmatrix} \dfrac{\Delta p_1}{p_1} \cdots \end{bmatrix}, \tag{A.12}$$

to formulate the optimization problem

$$\max \quad \boldsymbol{s}^{\mathrm{T}} \left(\sum \boldsymbol{\Omega}^{\mathrm{T}} \boldsymbol{\Omega} \Delta t \right) \boldsymbol{s}. \tag{A.13}$$

With scaling of the sensitivities

$$\boldsymbol{s}^{\mathrm{T}} \boldsymbol{s} = 1 \tag{A.14}$$

as additional constraint, the problem can be reformulated as an Euler–Lagrange equation with the solution

$$G\boldsymbol{s} = \lambda \boldsymbol{s}, \tag{A.15}$$

with

$$\boldsymbol{G} = \sum \boldsymbol{\Omega}^{\mathrm{T}} \boldsymbol{\Omega} \Delta\, t. \tag{A.16}$$

References

Agrawal, A., 1999. New institute to study systems biology. Nat. Biotechnol. 17, 743.

Barkai, N., Leibler, S., 1997. Robustness in simple biochemical networks. Nature 387.

Bergmeyer, H.U., 1979. Methoden der Enzymatischen Analyse. Verlag Chemie, Weinheim.

DeReuse, H., Danchin, A., 1988. The *ptsH*, *ptsI*, and *crr* genes of the *Escherichia coli* phosphoenolpyruvate-dependent phosphotransferase system—a complex operon with several modes of transcription. J. Bacteriol. 170, 3827–3837.

Francke, C., Westerhoff, H.V., Blom, J.G., Peletier, M.A., 2002. Flux control of the bacterial phosphoenolpyruvate: glucose phosphotransferase system and the effect of diffusion. Mol. Biol. Rep. 29, 21–26.

Hearne, J.W., 1985. Sensitivity analysis of parameter combinations. Appl. Math. Model. 9, 106–108.

Heinrich, R., Schuster, S., 1996. The regulation of cellular processes. Chapman & Hall.

Hogema, B.M., Arents, J.C., Bader, R., Eijkemanns, K., Yoshida, H., Takahashi, H., Aiba, H., Postma, P.W., 1998. Inducer exclusion in *Escherichia coli* by non-PTS substrates: the role of the PEP to pyruvate ratio in determining the phosphorylation state of enzyme IIA^{Glc}. Mol. Microbiol. 30, 487–498.

Ishizuka, H., Hanamura, A., Kunimura, T., Aiba, H., 1993. A lowered concentration of cAMP receptor protein caused by glucose is an important determinant for catabolite repression in *Escherichia coli*. Mol. Microbiol. 10, 341–350.

Kitano, H., 2000. Perspectives on systems biology. New Gen. Comput. 18 (3), 199–216.

Kremling, A., Gilles, E.D., 2001. The organization of metabolic reaction networks: II. Signal processing in hierarchical structured functional units. Metab. Eng. 3 (2), 138–150.

Kremling, A., Bettenbrock, K., Laube, B., Jahreis, K., Lengeler, J.W., Gilles, E.D., 2001a. The organization of metabolic reaction networks: III. Application for diauxic growth on glucose and lactose. Metab. Eng. 3 (4), 362–379.

Kremling, A., Sauter, T., Bullinger, E., Ederer, M., Allgöwer, F., Gilles, E.D., 2001b. Biosystems engineering: applying methods from systems theory to biological systems. In: Yi, T.-M., Hucka, M., Morohashi, M., Kitano, H. (Eds.), Proc. of the Second International Conference on Systems Biology, California Institute of Technology, Pasadena, CA, pp. 282–290.

Lee, S.J., Boos, W., Bouche, J.P., Plumbridge, J., 2000. Signal transduction between a membrane-bound transporter, PtsG, and a soluble transcription factor, Mlc, of *Escherichia coli*. EMBO J. 19, 5353–5361.

Liao, J.C., Hou, S.-Y., Chao, Y.-P., 1996. Pathway analysis, engineering, and physiological considerations for redirecting central metabolism. Biotechnol. Bioeng. 52, 129–140.

Ljung, L., 1999. System Identification—Theory for the User, 2nd ed. Prentice-Hall PTR, Upper Saddle River, NJ.

Palsson, B.O., Lightfoot, E.N. 1984. Mathematial modeling of dynamics and control in metabolic networks: I. On Michaelis–Menten kinetics. J. Theor. Biol. 111, 273–302.

Plumbridge, J., 1998. Expression of *ptsG*, the gene for the major glucose pts transporter in *Escherichia coli*, is repressed by Mlc and induced by growth on glucose. Mol. Microbiol. 29 (4), 1053–1063.

Posten, C., Munack, A., 1990. On-line application of parameter estimation accuracy to biotechnical processes. In: Proceedings of the American Control Conference, vol. 3, pp. 2181–2186.

Postma, P.W., Lengeler, J.W., Jacobson, G.R., 1993. Phosphoenolpyruvat: carbohydrate phosphotransferase systems of bacteria. Microbiol. Rev. 57, 543–594.

Rohwer, J.M., Meadow, N.D., Roseman, S., Westerhoff, H.V., Postma, P.W., 2000. Understanding glucose transport by the bacterial phosphoenolpyruvate:glycose phosphotransferase system on the basis of kinetic measurements in vitro. J. Biol. Chem. 275, 34909–34921.

Rojdestvenski, I., Cottam, M., Park, Y.I., Öquist, G., 1999. Robustness and time-scale hierarchy in biological systems. BioSystems 50, 71–82.

Schmid, K., Schupfner, M., Schmitt, R., 1982. Plasmid mediated uptake and metabolism of sucrose by *Escherichia coli*. J. Bacteriol. 151, 68–75.

Stelling, J., Klamt, S., Bettenbrock, K., Schuster, S., Gilles, E.D., 2002. Metabolic network structure determines key aspects of functionality and regulation. Nature 420, 190–193.

Takahashi, H., Inada, T., Postma, P., Aiba, H., 1998. CRP down-regulates adenylate cyclase activity by reducing the level of phosphorylated IIAGlc, the glucose-specific phosphotransferase protein, in *Escherichia coli*. Mol. Gen. Genet. 259, 317–326.

Tanaka, Y., Kimata, K., Aiba, H., 2000. A novel regulatory role of glucose transporter of *Escherichia coli*: membrane sequestration of a global repressor Mlc. EMBO J. 19, 5344–5352.

Wang, J., Gilles, E.D., Lengeler, J.W., Jahreis, K., 2001. Modeling of inducer exclusion and catabolite repression based on a PTS-dependent sucrose and non-PTS-dependent glycerol transport systems in *Escherichia coli* K-12 and its experimental verification. J. Biotechnol. 92, 133–158.

Wohlieter, J.A., Lazare, J.R., Snellings, N.J., Johnson, E.M., Syneki, R.M., Baron, R.S., 1975. Characterization of a transmissible genetic element from sucrose fermenting samonella strains. J. Bacteriol. 122, 401–406.

Zeppenfeld, T., Larisch, C., Lengeler, J.W., Jahreis, K., 2000. Glucose transporter mutants of *Escherichia coli* K-12 with changes in substrate recognition of the $IICB^{Glc}$ and induction behavior of the *ptsG* gene. J. Bacteriol. 182, 4443–4452.